Dehydrogenation by Heterogeneous Catalysts

Daniel E. Resasco

School of Chemical Engineering and Materials Science

University of Oklahoma

Encyclopedia of Catalysis

January, 2000

1. INTRODUCTION

Catalytic dehydrogenation of alkanes is an endothermic reaction, which occurs with an increase in the number of moles and can be represented by the expression

$$\text{Alkane} \Leftrightarrow \text{Olefin} + \text{Hydrogen}$$

This reaction cannot be carried out thermally because it is highly unfavorable compared to the cracking of the hydrocarbon, since the C-C bond strength (about 246 kJ/mol) is much lower than that of the C-H bond (about 363 kJ/mol). However, in the presence of a suitable catalyst, dehydrogenation can be carried out with minimal C-C bond rupture. The strong C-H bond is a closed-shell σ orbital that can be activated by oxide or metal catalysts. Oxides can activate the C-H bond via hydrogen abstraction because they can form O-H bonds, which can have strengths comparable to that of the C-H bond. By contrast, metals cannot accomplish the hydrogen abstraction because the M-H bonds are much weaker than the C-H bond. However, the sum of the M-H and M-C bond strengths can exceed the C-H bond strength, making the process thermodynamically possible. In this case, the reaction is thought to proceed via a three centered transition state, which can be described as a metal atom inserting into the C-H bond. The C-H bond bridges across the metal atom until it breaks, followed by the formation of the corresponding M-H and M-C bonds.[1] Therefore, dehydrogenation of alkanes can be carried out on oxides as well as on metal catalysts. In fact, both types of dehydrogenation catalysts are typically found in a number of important industrial applications.

Catalytic dehydrogenation is employed in the production of propylene and isobutylene from propane and isobutane, in the production of C_6 to C_{19} mono-olefins from the corresponding normal alkanes, and of styrene from ethylbenzene. In this

contribution, the chemistry involved in these reactions will be discussed, with particular emphasis on the effects of catalyst structure and composition on the catalytic properties.

2. THERMODYNAMIC EQUILIBRIUM LIMITATIONS

The dehydrogenation reactions are thermodynamically favored at high temperatures and low pressures. The equilibrium conversion can be readily calculated by the expression:

$$K_p = \frac{x \quad (\mathbf{h} + x) \quad P}{(1 - x) \quad (1 + \mathbf{i} + \mathbf{h} + x)} \qquad (1)$$

where K_p is the equilibrium constant, x the equilibrium conversion, **i** and **h** the number of moles of inerts and hydrogen, per mole of alkane in the feed, respectively. The equilibrium conversion for the dehydrogenation of propane as a function of temperature is illustrated in Fig. 1 for typical hydrogen/alkane (**h**) and inert/alkane (**i**) feed ratios. In some industrial operations, part of the hydrogen produced is recycled to inhibit the formation of coke on the catalyst. However, at a given temperature, the equilibrium conversion decreases with the hydrogen/alkane feed ratio. For example, under typical dehydrogenation conditions (550ºC, 1 atm) the equilibrium conversion decreases from about 44 % to 25 % when the H_2/alkane ratio increases from 0 to 3. Therefore, the hydrogen/alkane feed ratio is a compromise between coke suppression and conversion. Contrarily, when inerts, such as steam or nitrogen, are added to the feed the equilibrium is benefited. For example, if the inert/alkane ratio is increased from 0 to 3 at 550ºC and 1 atm, the equilibrium conversion increases from 44 % to 64 %.

3. CATALYTIC DEHYDROGENATION OF ISOBUTANE AND PROPANE

The catalytic dehydrogenation of isobutane and propane are important reactions used commercially for the production of isobutylene and propylene, respectively. One of the major applications of isobutylene is as a feedstock in the manufacture of methyl tertiary butyl ether (MTBE). In the United States, MTBE has been used in relatively low concentrations as an octane booster in gasoline for more than 25 years. However, since 1992, it has been used in high concentrations in a large number of cities, to meet requirements of the Clean Air Act in the oxygenated and reformulated gasolines. In those cases, up to about 15 % MTBE is added to gasoline to allow more complete combustion and reduce emissions of carbon monoxide (CO) and volatile organic compounds (VOC). In recent years, objections to potential health effects of MTBE caused by water contamination have arisen, which may have an impact on the MTBE demand.[2] However, demand for polyisobutylene, and polybutenes in general, is in continuous growth. Thus, the needs for C_4 olefin production will probably remain high. C_4 olefins are mainly produced from FCC (about 50 %) and steam cracking (21 %). However, in some industrial operations, it is necessary to have increased flexibility in the olefin supply and so, production of a single specific alkene is sometimes required. In those cases, the direct catalytic dehydrogenation is the ideal solution. Propylene is an important basic chemical building block for plastics and resins. Its worldwide demand has steadily grown for the last 15 years and it is projected that, in the coming years, demand growth for propylene will be equal to or even higher than that for ethylene.[3] Similar to isobutylene, propylene can be produced as a by-product from FCC and steam

cracking operations. However, in response to the growing demand and for the greater flexibility in the olefin pool that a dedicated process has in comparison to cracking units, several propane dehydrogenation plants are now being operated in the world.

The dehydrogenation of lower alkanes is typically carried out on two different types of catalysts: a) Pt-based catalysts and b) chromia-based catalysts.[4-6] The main characteristics of these two types of catalysts will be discussed here, together with some reference to other less common materials. Several commercial processes for dehydrogenation of lower alkanes are currently available. The severely deactivating conditions imposed by the dehydrogenation process have challenged the process designers to develop efficient reactors for this difficult task. Several options have been tested and several have found successful applications. Among the various commercial processes available for dehydrogenation of propane and isobutane, one can find fixed bed reactors, operated in isothermal or adiabatic form. Some include cyclic operations, others include continuous catalyst regeneration with moving beds, or with fluidized beds.

3.1. Pt-based dehydrogenation catalysts:

A side reaction that frequently competes with dehydrogenation is hydrogenolysis. Platinum is a primary component in many dehydrogenation catalysts due to its high activity for activating C-H bonds, coupled with an inferior activity for the rupture of C-C bonds, resulting in intrinsically high selectivities toward dehydrogenation. On a Pt surface, only low-coordination number sites (steps, kinks) are able to catalyze the C-C bond breaking, while essentially all Pt sites catalyze the rupture of the C-H bonds.

Another undesired side reaction that competes with dehydrogenation is coke formation. Since both, hydrogenolysis and coke formation, are more sensitive to the support structure than dehydrogenation, any impurity or inactive species on the surface may act as a site diluent and should increase the selectivity toward dehydrogenation. This effect is well documented and has been observed in a number of bimetallic systems.[7, 8] In addition to the dilution of sites, other more subtle factors may play a role in altering the activity of the Pt surface. For example, significant differences in the magnitude of these effects have been detected in a series of Pt catalysts promoted by the addition of different metals, which are themselves inactive, such as Sn, In, Pb, and Cu, but can alter the properties of Pt.[9] It was found that the promoting effect among these metals was highest from the addition of Sn and lowest from Cu. In fact, Sn has been the preferred promoter for most Pt dehydrogenation catalysts.[10, 11] In section 3.1.2, we discuss the effects of Sn in greater detail.

3.1.1. Reaction Mechanism and Kinetics on Pt Catalysts

The isobutane dehydrogenation on Pt-based catalysts has generally been described by the following set of reaction steps:

(A) $C_4H_{10} + 2\,* \Leftrightarrow C_4H_9* + H\,*$

(B) $C_4H_9* + 2\,* \Leftrightarrow C_4H_8** + H\,*$

(C) $C_4H_8** \Leftrightarrow C_4H_8 + 2\,*$

(D) $H_2 + 2\,* \Leftrightarrow 2\,H*$

Cortright et al.[12] have conducted deuterium tracing studies under reaction conditions, which showed a much larger extent of deuterium in the isobutylene product

than in the isobutane. Also, it was seen that the small fraction of isobutane that contained deuterium was fully deuterated, indicating that the dissociative adsorption of isobutane is slow compared to the exchange of hydrogen/deuterium in the adsorbed isobutyl species. These results support the hypothesis that step (A) is the slowest step and are in line with earlier observations that show that as the hydrogen pressure increases, the dehydrogenation rate decreases as a result of the competition of hydrogen and the alkane for adsorption sites.[13] Accordingly, the following rate expression should represent the kinetics

$$r_D = k_A \theta_*^2 \left[P_{iC4H10} - \left(P_{iC4H8} P_{H2} \right) / K_{eq} \right] \qquad (2)$$

where r_D is the net dehydrogenation rate, k_A is the rate constant for the dissociative adsorption of isobutane (step A), K_{eq} is the overall equilibrium constant for isobutane dehydrogenation, and θ_* is the fraction of sites free of adsorbed species. The isobutane coverage under reaction conditions is practically negligible[12] and the fraction of free sites can be determined from a expression derived from the assumption that the only species on the surface are hydrogen and isobutylene, which are in equilibrium with the gas phase. Accordingly the expression for the fraction of free sites can be expressed as:

$$\theta_* = \frac{-K_C}{4P_{iC_4H_8}}\left[1+\sqrt{K_D P_{H_2}}-\sqrt{1+2\sqrt{K_D P_{H_2}}+K_D P_{H_2}+\frac{8P_{iC_4H_8}}{K_C}}\right] \qquad (3)$$

where K_C and K_D are the equilibrium constants for isobutylene desorption (step C) and hydrogen adsorption (step D) , respectively. Combining equations (2) and (3) excellent fits have been obtained on a number of reaction data over a wide range of

temperatures, concentrations, and catalysts.[14] All the fitting parameters thus obtained had physical meaning and were used to compare thermodynamic functions on different catalysts. This kinetic expression clearly explains the reaction orders obtained on most previous studies, i.e., first order dependence with respect to the alkane and negative half to zeroth order dependence in hydrogen.[9, 13]

3.1.2. Addition of Sn to Pt as a promoter for activity, selectivity, and catalyst life

The addition of Sn has important beneficial effects on the catalytic properties of Pt for the dehydrogenation of lower alkanes. First of all, and as mentioned above, it increases the selectivity towards dehydrogenation by inhibiting hydrogenolysis. Similarly, the addition of Sn has a profound effect on the catalyst life. The Pt-Sn catalyst retains a much higher activity than the pure Pt catalyst. The enhancement in selectivity and stability, clearly illustrated in Fig. 2a and 2b, can be explained in geometric terms by the dilution of Pt ensembles by Sn. As described above, this dilution greatly reduces the activity towards reactions that require a large ensemble of Pt atoms to constitute the active sites, such as hydrogenolysis and coking. Also, the increase in selectivity of the pure Pt sample with time on stream shown in Fig. 2b can be explained by the same geometric arguments. The carbon deposited during the reaction plays the role of an inactive species that inhibits undesired reactions, including coking. This explanation accounts for two observations on the pure Pt catalyst. Both, the selectivity and the stability of the catalyst improve as a function of time on stream as the number of large ensembles is reduced by the presence of carbon. On the pure Pt catalyst the initial deactivation is very fast. Thus, it is difficult to measure the true initial activity of unpromoted Pt and determine whether the initial dehydrogenation rate on Pt is higher or

lower than on the bimetallic catalyst. In fact, pure Pt may be initially more active, but after a short time it deactivates while the bimetallic retains its activity. This phenomenon is particularly pronounced in the absence of added H_2, as in the experiments of Fig. 2. The higher initial activity of pure Pt catalysts can only be observed when high H_2/hydrocarbon feed ratios are employed.[15]

3.1.3. Preparation of Pt-Sn Dehydrogenation Catalysts and its effects on performance

The beneficial role of adding Sn to Pt catalysts has been observed on different supports and on catalysts prepared by various methods. In some preparations the addition of Sn has been conducted by sequential impregnation, first of an aqueous solution containing the Sn precursor (typically $SnCl_2$) and then of another solution containing the Pt precursor (typically H_2PtCl_6). In these preparations, the degree of Pt-Sn interaction is relatively low because Sn tends to interact with the support becoming segregated from Pt. Therefore, to maximize the metal-metal interaction, other preparations have been used. For example, the use of an aqueous solution containing both Pt and Sn precursors and excess HCl results in the formation of a bimetallic $PtCl_2(SnCl_3)_2^{2-}$ complex.[16,17] In this preparation, both metals are deposited on the surface in the same compound and, after the thermal treatment, a high degree of alloyed metals can be obtained. Other methods involve the Pt-catalyzed surface reduction of an organometallic tin compound, resulting in the selective deposition of Sn over the Pt surface.[18] For example, the catalyst can be prepared from a solution of $Sn(C_4H_9)_4$ in an organic solvent, such as *n*-hexane. This solution is added onto a pre-reduced Pt/support sample, without exposure to air. The H

that remains adsorbed on Pt is responsible for the reduction of the $Sn(C_4H_9)_4$, causing the selective deposition over the metal.[19]

The catalyst preparation may critically influence the Pt-Sn interaction and consequently the catalytic behavior. As illustrated in Fig. 3 for a series of Pt-Sn catalysts supported on silica, the promoting effect of Sn strongly depends on the method employed in the preparation. Catalysts prepared by co-impregnation, particularly when the solvent is an aqueous solution containing HCl, result in a relatively high extent of Pt-Sn interaction. By contrast, sequential impregnation results in a large fraction of unalloyed Pt.

Although alumina and silica have been the two supports most widely studied for dehydrogenation reactions, other non-acidic supports have also shown promising properties. For example, KL zeolite has been proposed to be an effective support for Pt-Sn dehydrogenation catalysts. It has been reported[20] that these catalysts maintain high isobutane dehydrogenation activity and selectivity for extended reaction intervals. Characterization of these materials indicates that a fraction of the Sn is alloyed with Pt and the rest is in the form of Sn^{2+} ions, exchanged with K^+ previously present in the zeolite. It was further hypothesized that the K displaced from the zeolite framework can interact with the Pt-Sn alloy particles, promoting the activity. The promoting effect of K was demonstrated by deliberate addition of excess K to the catalysts, which greatly enhanced the dehydrogenation activity and selectivity.

Table 1 makes a comparison of the isobutane dehydrogenation conversion on several Pt and Pt-Sn catalysts.[20] In the table we compare the reaction rates per gram of Pt. It is generally accepted that the best form of comparing the activity of a series of

catalysts is in terms of turnover frequency (TOF), based on the number of sites as measured by hydrogen chemisorption. However, when Pt-Sn alloys and unalloyed Pt phases co-exist, the TOF may be misleading. The chemisorptive capacity of Pt is greatly changed when it is alloyed with Sn. For example, it has been shown that the heat of CO adsorption drops from Pt to PtSn alloy by as much as 20 kJ/mol.[21] This energy difference causes significant changes in the adsorption equilibrium constants at 298 K and, consequently, in the observed adsorption capacity. In recent work,[22] it was observed that the CO adsorption capacity of Pt-Sn/SiO_2 dropped to zero after 1 hour at 500ºC on isobutane stream. However, the catalyst was almost as active for dehydrogenation as at the beginning of the reaction. The reason for this apparent discrepancy is that the unalloyed Pt is rapidly covered by coke, while the Pt-Sn alloys remain more or less free of coke. Since alloyed Pt does not adsorb significant amounts of CO the CO/Pt measured on the fresh catalyst was mainly due to the fraction of unalloyed Pt, which after a while contributes little to the activity. The situation is very similar for the chemisorption of hydrogen. Verbeek and Sachtler[23] have shown that Pt-Sn alloys adsorb very little hydrogen and have ascribed this decrease to a lowering of the heat of adsorption. Microcalorimetry studies[24] have shown that, even though the addition of Sn resulted in a large decrease in the saturation adsorption coverages for H or CO, the heats of adsorption at zero coverage on Pt:Sn samples were similar to those on pure Pt. However, it must be noted that these SiO_2-supported samples were prepared by sequential impregnation and, as shown below, this technique leads to a large fraction of unalloyed Pt, which may be responsible for the measured high heats of adsorption. For changes in the initial heats of adsorption to be seen, the majority of Pt needs to be alloyed with Sn. In fact, when

higher Sn concentrations were used in those studies,[24] the heats of adsorption at zero coverage decreased significantly, in agreement with the idea mentioned above. Only at very high H_2/hydrocarbon ratios, at which the deactivation is less pronounced, the TOF values for Pt and Pt-Sn catalysts are normally found to be similar. It is generally observed that the initial deactivation increases with the amount of unalloyed Pt, then the unalloyed Pt in the sample is not related to the catalytic activity. However, CO and H_2 chemisorption primarily occurs on the unalloyed Pt. Therefore, for bimetallic Pt-Sn catalysts, we prefer to report rates per total Pt.

A different methodology to estimate TOF has been proposed by Rajeshwer et al.[25] These authors propose that hydrogen/oxygen titration on Pt-Sn alloys is an activated process and, as a result, the hydrogen titration of preadsorbed oxygen conducted at room temperature only reflects the exposed fraction of unalloyed Pt, but that conducted at 150ºC titrates both alloyed and unalloyed Pt. As a result, the difference between the two uptakes reflects the exposed fraction of alloyed Pt. This is an interesting method, although the possibility of hydrogen spillover onto the support,[26] may lead to overestimation of the density of alloyed Pt. To rule out this possibility, Rajeshwer et al. conducted measurements on physical mixtures of monometallic Pt and Sn catalysts, which showed the same uptake as the monometallic Pt catalyst. However, values of H/Pt uptake ratios much greater than one have sometimes been observed, which is hard to explain without invoking spillover onto the support or, as suggested by some authors, hydrogen uptake by dissolution in the bulk of the Pt-Sn alloys. [23]

3.1.4. Structure and Composition of Pt-Sn Catalysts

The assessment of Pt dispersion on monometallic catalysts and quantification of its exposed sites is well established and can be readily accomplished by standard techniques such as hydrogen chemisorption, electron microscopy, or EXAFS. As described in the previous section, the same task is much less straightforward with bimetallic Pt-Sn catalysts. Pt and Sn are able to form a number of ordered Pt-Sn alloys, such as PtSn, $PtSn_2$, $PtSn_4$, Pt_2Sn_3, and Pt_3Sn.[27]

However, the formation of alloys like these on high-surface-area supports strongly depends on the nature of the support, thermal treatments, impregnation method, anions present, etc. In addition, the chemisorptive properties of these alloys are less understood than those of pure Pt. Another fundamental question related to these systems is the oxidation state of Sn under reaction conditions. Upon reduction, tin may remain in the Sn^{II} or Sn^{IV} forms or may get reduced to the metallic Sn^0 state and form Pt_xSn_y alloys.

Pt-Sn alloys are more easily formed when the support interacts only weakly with the Pt and Sn, such as in the case of silica-supported catalysts. One of the techniques commonly employed to determine the oxidation state of supported metals and identify metal-metal interactions is temperature programmed reduction (TPR). Fig. 4 shows the TPR of a bimetallic Pt-Sn/SiO_2 catalyst compared to a monometallic Pt/SiO_2 catalyst after calcination at 350ºC.[22] The TPR for the pure Pt catalyst shows a H_2 consumption peak at about 125°C. The profile for the bimetallic Pt-Sn catalyst has two H_2 consumption peaks. The first one appears in the same position as that for pure Pt (125°C), while the second has a maximum at 200°C. This peak is associated with the reduction of a Pt-Sn alloy. EXAFS studies[28] conducted on the same set of samples

confirm that the bimetallic Pt-Sn/SiO_2 catalyst has both unalloyed Pt and alloyed Pt-Sn. Fig. 5 shows that the radial distribution of the bimetallic sample clearly exhibits two peaks. However, as shown in the simulated data of Fig. 6, neither the pure Pt or the PtSn alloy alone exhibits those peaks. Only when both Pt and PtSn coexist is that the two peaks appear. Therefore, the presence of the two peaks in the radial distribution of the Pt-Sn/SiO_2 catalyst demonstrates the presence of both unalloyed Pt and PtSn alloy. The fitting of the experimental data indicated that, in that sample 35 % of the Pt was unalloyed, and 65 % in the form of the PtSn alloy. Using other alloys, such as Pt_3Sn and $PtSn_2$ resulted in poor fits. Similar conclusions were obtained from Mössbauer spectroscopy and X-ray diffraction data.[29] These results indicate that, on silica support, PtSn alloy is formed upon reduction in hydrogen. By contrast, when alumina is used as a support, the reduction of Sn to the metallic state is much more difficult. Studies of Pt-Sn/Al_2O_3 catalysts with tin loadings in the range 0.3 – 5.0 wt % showed no evidence of metallic tin, even after reduction at high temperatures. Only when the tin loading is increased to very high values, a small fraction of metallic tin can be obtained. Fig. 7 shows XPS data of a Pt-Sn/SiO_2 (5 wt % Pt, 5 wt % Sn) catalyst and a Pt-Sn/Al_2O_3 (5 wt % Pt, 29 wt % Sn) catalyst.[30] It is observed that, even with such a high Sn loading, the fraction of metallic Sn is low compared to that obtained on silica.

3.1.5. Is the Sn promotion of Pt geometric or electronic in nature ?

The arguments in favor or against geometric or electronic effects have captured the attention of Heterogeneous Catalysis researchers for decades. Today, it is widely accepted that if a given metal of very low catalytic activity is distributed uniformly over

the surface of a more active metal, the activity of the active metal is greatly affected for reactions requiring a large ensemble of atoms, but it is only moderately affected for reactions that require a single site. This effect can be explained by simple geometric dilution of the active sites by the presence of the inactive atoms. However, the question that still generates controversy is whether the atoms of the active metal that remain exposed to the gas phase are chemically (or electronically) altered by the presence of the inactive metal. In many cases, the electronic modification of the active species is very small compared to the more notable geometric effect. For example, large activity losses are typically observed for the ethane hydrogenolysis on Ni when small amounts of Cu are added to the catalyst. However, much lower effects are observed on the same catalysts for the dehydrogenation of cyclohexane[31]. In that case, geometric effects are clearly dominant and only small effects could be attributed to an electronic modification of Ni by the presence of Cu.

In Pt-Sn alloys, both geometric and electronic effects seem to play significant roles. An evidence in support of electronic modifications of Pt by the presence of Sn can be obtained by X-ray Absorption Near-Edge Spectroscopy (XANES), which is usually considered a good technique to probe the electronic state of an atom in its environment. In the L_{III} XANES spectra, the so-called "white line" feature is a prominent pre-edge maximum that shows significant variations with changes in the oxidation state of the metal. Among the various contributions to absorption in this region, the most important one is an intra-atomic p-to-d electronic transition, from occupied *2p* states to unoccupied *5d* states in the central Pt atom. An oxidized Pt sample has a higher density of unoccupied d states and, as a result, the white line notably increases in comparison to that

of the metallic Pt. Accordingly, an alteration of the Pt L_{III} edge shape caused by addition of Sn would indicate an electronic modification of Pt, caused by the presence of Sn. This alteration has, in fact, been reported in several papers, and it is illustrated in Fig. 8. The reduction in the of the white line intensity has been taken by some authors as an indication of a decrease in the density of unoccupied *d* states in Pt, which means that an electron transfer occurs from Sn to Pt. Other authors[32] have postulated that the intermetallic interaction may involve *sp* orbitals. The Pt-Sn bonding in Pt_3Sn alloys would involve the occupied Sn *5p* and the unoccupied Pt *6sp*. The resulting donation of *p* electrons from Sn to Pt would only have an indirect effect on the *d* states of Pt.

Recent quantum chemical calculations support these results and show that Sn donates electrons to both *6sp* and *5d* orbitals. These calculations used density functional theory (DFT) and were conducted for two types of Pt and Pt-Sn clusters. In the first type, 19 Pt atoms were constrained in three layers of an FCC-like crystal configuration, keeping a fixed interatomic distance of 2.77Å. To study the effect of Sn, three Pt atoms were replaced in the corners of the top layer. These two clusters were called Pt_{19} and $Pt_{16}Sn_3$, respectively. In the second type of cluster, the distribution of 10 Pt atoms was optimized for energy minimization, letting the interatomic distances relax from the bulk value of 2.77Å. Here, the effect of Sn was evaluated by replacing four Pt atoms by Sn atoms, three at the corners of the top layer, and one at the bottom. Table 2 summarizes the Mulliken electron population of the *6s, 6p*, and *5d* orbitals in three top Pt atoms for the four different clusters. A clear increase in electron population is observed in both the *6sp* and *5d* orbitals when Sn is added in the cluster, indicating an electron donation from Sn to Pt.

Even when electronic interactions do occur, they may not necessarily have significant effects on the catalytic properties. The analysis of the nature and energetics of adsorption of certain adsorbates may help determine whether electronic effects have important influences in catalysis. For example, in the Pt-Sn system, the adsorption of ethylene has been a sensitive probe that has provided important information.[33] It is known that on pure platinum, ethylene can adsorb in different forms. At low temperatures, π-bonded ethylene and di-σ bonded ethylene species can be observed. However, as the temperature is increased above room temperature, an ethylidyne species appears. The evolution of these species as a function of temperature can be examined in the following IR and microcalorimetry experiments. As shown in the IR spectra in Fig. 9, when the adsorption of ethylene is conducted on a Pt/SiO_2 catalyst at –70ºC, two bands are typically observed at 1506 and 1428 cm^{-1}. These bands are due to π-bonded ethylene and di-σ-bonded ethylene, respectively. Under these conditions, the measured initial heat of adsorption is 125 kJ/mol. By contrast, when the temperature is increased to room temperature (25ºC), the bands at 1506 and 1428 cm^{-1} almost completely disappear and a new band at 1342 cm^{-1} dominates the spectrum. This band is due to ethylidyne. At this temperature, the initial heat of adsorption increases to 157 kJ/mol, consistent with a stronger interaction of the ethylidyne species with the surface. A different behavior is observed on the $Pt\text{-}Sn/SiO_2$ catalyst. For this catalyst, the same two bands at 1506 and 1428 cm^{-1} are observed at low temperatures, but they do not disappear when the temperature is increased to 27ºC. At this temperature, the transformation of π-bonded ethylene and di-σ-bonded ethylene species to ethylidyne is much less pronounced on the bimetallic catalyst than on the pure Pt catalyst. Then, not only the bands corresponding

to π-bonded ethylene and di-σ-bonded ethylene species are more intense, but also the band corresponding to ethylidyne is significantly weaker than on pure Pt. As mentioned above, it is possible that a significant fraction of Pt remains as unalloyed Pt. Therefore, the small ethylidyne band observed on the Pt-Sn catalyst may in fact be due to adsorption sites on the small Pt fraction that is not alloyed with Sn. The microcalorimetric data on the Pt-Sn catalysts are also consistent with the IR data. The observed heat of adsorption at room temperature was only 135 kJ/mole, much lower than on pure Pt, which was 157 kJ/mol. The observed hindrance in the ability of Pt to form the ethylidyne surface species when Sn is added could just be due to a geometric blockage by Sn of the 3-fold Pt sites necessary to stabilize the ethylidyne species. In fact, that may certainly occur. However, the DFT quantum chemical calculations have shown that, even when Sn is not occupying the 3-fold Pt sites, it may exert an electronic effect that prevents the stabilization of ethylidyne. The calculated changes in energy, per mole adsorbed, when π-bonded ethylene, di-σ-bonded ethylene, or ethylidyne species form on Pt and Pt-Sn clusters are summarized in Table 3. It is observed that the addition of Sn weakens the interaction of ethylene with Pt for all three species. However, the effect is most pronounced for the ethylidyne species. On the Pt-Sn clusters, very small, if any, exothermicity is predicted by these calculations for the adsorption on the 3-fold Pt sites. Moreover, the Mulliken population analysis suggests that the formation of ethylidyne species on Pt involves electron donation from ethylidyne to the *6sp* orbitals on Pt, accompanied by back-donation from the *5d* orbitals to the adsorbate. This analysis further shows that the increased electronic population in Pt as a result of the addition of Sn, causes a more repulsive interaction for the formation of ethylidyne than for the formation of π-bonded

ethylene or di-σ-bonded ethylene. Therefore, it seems that when Sn is added to Pt, both geometric and electronic effects contribute to inhibit the stabilization of ethylidyne on the surface.

3.1.6. Catalyst Deactivation and Regeneration

The major cause of catalyst deactivation in dehydrogenation processes is carbon deposition. The high temperatures and low pressures necessary to achieve high equilibrium conversions are conducive to the rapid formation of coke. The use of promoters and the operating conditions, e.g., temperature and H_2/alkane ratio, are parameters that can be adjusted to modify the rate and extent of carbon deposition.

A typical kinetics expression that describes the rate of carbon formation has the form:

$$r_C = \frac{k_1 P_{iC4H8} - k_{-1} P_H^2 C}{(1 + K_a P_{iC4H8} + K_b P_H^{1/2} + K_c C)} \qquad (4)$$

where P_{iC4H8} and P_H are the partial pressures of olefin and hydrogen, respectively, C is the concentration of carbon on the surface, and k_1, k_{-1}, K_a, and K_b temperature-dependent parameters that are a function of the catalyst. Here it is important to note that the expression predicts a strong inhibition of coke formation by both a negative term in the numerator, which reflects the elimination of carbonaceous deposits by hydrogenation and a term in the denominator that result from the competition for adsorption sites. The expression also predicts that the rate of coke formation is expected to be higher initially, when the amount of carbon on the surface is low. Both trends are in fact observed experimentally. What is important to discuss is that the concentration at which the

carbon on the surface begins to inhibit further deposition is a strong function of the catalyst composition. For example, while on a Pt/Al_2O_3 catalyst, the rate of formation starts slowing down at a carbon content of about 2 wt % C, on a bimetallic $Pt\text{-}Sn/Al_2O_3$ catalyst the coking rate remains unchanged up to about 7 wt % C.

Due to the substantial formation of coke, lower alkane dehydrogenation catalysts require frequent regenerations. Different regeneration procedures have been tested, the most common ones involving oxygen, but other alternative, or complementary methods involve treatment in chlorine, steam or sulfur-containing streams.[34] The most obvious effect of the regeneration treatment with oxygen is the burning of the carbonaceous deposits. It is generally accepted that two distinct coke burning processes occur as a function of temperatures. Oxidation of carbonaceous deposits is a catalytic process that is greatly accelerated by Pt, or other metals typically used in dehydrogenation reactions. Therefore, the oxidation of coke in contact with (or in the close vicinity of) the metal particles can readily occur at relatively low temperatures. By contrast, the coke deposited on the support, away from the metal particles, can only be oxidized at high temperatures because it requires the spillover of activated oxygen from the metal onto the support.

The two oxidation regions can be clearly demonstrated by the temperature programmed oxidation (TPO) technique. When the support is alumina two distinct oxidation peaks are clearly observed, one at about 450°C and another above 500°C. A clear demonstration that the one at the lower temperature is associated with the metal was conducted on Pt and Pt-Sn catalysts.[35] Both, the dehydrogenation activity and hydrogen chemisorption capacity were completely restored after a partial oxidation of the coke deposits at 450°C. These results clearly demonstrate that the coke removed by high

temperature oxidation is located on the support, rather than on the metal. A second important result obtained in the same investigation was the demonstration that the relative amounts of each of the two types of coke is a strong function of the Sn/Pr ratio in the catalyst.[35] As illustrated in Fig. 10, an increase in the amount of Sn causes not only a decrease in the amount of coke on the metal but also an increase in the amount of coke on the support, indicating that the presence of Sn enhances the mobility of coke, or its precursors, from the metal to the support.

In addition to the burning of coke, other secondary undesired effects may also occur during the treatment in oxygen. For example, although at intermediate temperatures in the presence of oxygen, sintering is relatively slow, at the high temperatures required to completely eliminate the coke, rapid growth of Pt particles occurs. The reason for this is that at the intermediate temperatures (e.g., around 400C) Pt is in the oxide form, which interacts with the oxidic support, slowing down the Pt mobility. However, above 500C, Pt oxide becomes unstable and metallic Pt is more susceptible to sintering.

The oxidation treatment not only may cause metal sintering but it can also alter the interaction between the metal and promoter due to a disruption between Pt and Sn that tends to occur under oxidation conditions. For example, temperature programmed reduction (TPR) studies of sequentially impregnated Pt-Sn/SiO_2 catalysts, treated in air at increasing temperatures and increasing periods of time, showed that the H_2 consumption peak associated with the reduction of Pt-Sn alloys, significantly decreased while those ascribed to unalloyed Pt and unalloyed Sn increased. This trend can be explained in terms of a segregation of the Pt and Sn caused by the high temperature oxidation. As

illustrated in the TPR of Fig. 11, the segregation was also observed in co-impregnated catalysts, which started with a much higher extent of Pt-Sn interaction. The fresh catalyst exhibited H_2 consumption peaks at about 146 and 186ºC, which correspond to Pt-Sn phases richer in Pt and Sn, respectively. After an oxidation treatment conducted at 500ºC to eliminate the coke formed during reaction, the peaks clearly split, generating a peak at 125ºC, which corresponds exactly to the reduction of unalloyed Pt, and a broader peak centered at about 240ºC, which can be ascribed to bimetallic phases rich in Sn. TEM evidence also supports the proposed segregation phenomenon. TEM studies on model Pt-Sn catalysts,[36] have shown that oxidation at 550ºC for 1 hour resulted in severe morphological changes in the intermetallic particles. The Sn in the alloys formed an oxide and migrated to the surface of the particle. SnO_2 formed a ring around the edge of the particle in contact with the SiO_2 support. The Pt did not form an oxide but became metallic Pt at the core of the particle. Subsequent 18 hour reduction (650ºC) resulted in complete recombination of the alloys.

An important point to discuss is whether the disruption of the alloys and segregation phenomena have significant effects on catalytic properties. Experimental results show that, in fact, the effects may be very large. As shown in Fig. 12, the oxidative regeneration treatment results in an important drop in conversion, together with a much higher propensity of the catalyst to form coke. As compared in the TPO profiles of Fig. 13 for a Pt-Sn/SiO_2 sample, after the first run and after an oxidation./reduction cycle followed by reaction. A much greater amount of carbon was produced on the catalyst that had been subjected to the oxidation/reduction regeneration treatment. Note that on silica-supported catalysts only one TPO peak is observed, as opposed to the

alumina-supported catalysts described in Fig. 10, where one peak corresponds to coke on the metal and one on the support. Therefore, all the coke formed in this case must be associated with the metal. When the comparison is made between Pt-Sn bimetallic catalysts and pure Pt catalysts, it is observed that the latter forms much more coke, and the TPO peak appears at somewhat higher temperatures, due to a more refractory nature of the carbon. In the case of the Pt-Sn sample, after the oxidation/reduction cycle, the TPO peak shifts to the same position as that observed on pure Pt catalysts. This shift indicates that some of the alloy has been destroyed, leaving behind patches of unalloyed Pt, on which the formation of the graphitic carbon is more favorable. The regenerated Pt-Sn catalyst still form less carbon than the pure Pt sample, but almost four times the amount found on the fresh bimetallic sample. Therefore, the activity loss observed after the oxidation/reduction cycle can be linked to the partial destruction of the Pt-Sn alloy, which results in an increase in the deactivation due to coking. Under oxidizing conditions at high temperatures, the Sn forms an oxide and, at the expense of the subsurface layer, the exterior becomes rich in Sn. The Pt, which does not form an oxide, is metallic and becomes the core of the particle. Reduction at high temperatures results in the destruction of the oxide and possibly redistribution of the Sn, opening patches of pure Pt. Although the thermodynamically most stable configuration is the complete recombination of the alloy, short reduction times do not allow for this to occur. Consequently, after the oxidation/reduction cycle, the bimetallic particles have become heterogeneous, with Sn-rich regions interdispersed with Pt-rich regions. It is even possible that pure Pt ensembles are present allowing for the formation of more refractory carbon to form on the surface under subsequent exposure to reaction conditions. On

alumina-supported catalysts, the disruption of Pt-Sn alloys by the high temperature oxidation is even more pronounced than on silica-supported catalysts.[37]

The deleterious effects of alloy disruption and Pt-Sn segregation, as well as sintering of Pt may be overcome by the so-called oxychlorination treatment. In this treatment chlorine-containing compounds are incorporated in the oxidation stream. This is a process that has been employed for many years in the regeneration of naphtha reforming catalysts, but has also been applied in the regeneration of dehydrogenation catalysts. With monometallic Pt catalysts, the main effect of the oxychlorination treatment is the redispersion of the Pt particles, which may have sintered during the coke burning operation. During the oxychlorination treatment, volatile Pt oxychloride species form and effectively re-disperse the Pt when these species are anchored by the alumina support. When Sn is present on the catalyst, the effect of chlorine during the oxidation/reduction cycles depends on the type of support and the Sn loading. For example, on alumina, Sn may block the anchoring sites of the support, thus inhibiting the redispersion process. But, at the same time, oxychlorination of bimetallic Pt-Sn catalysts enhances the contact between Pt and Sn. Thus Cl may have the effect of minimizing the Pt-Sn segregation that would normally occur in the oxidation treatment without chlorine.[38] The unwanted effect of the oxychlorination process is the generation of acidity on the support, which must be neutralized to avoid the increase in coke formation and isomerization products in the subsequent cycle.

Other regeneration methods include the use of steam, either during the regeneration or continuously during the reaction. Steam can help to reduce the formation of coke, via the reaction:

$$C + 2\,H_2O \Leftrightarrow CO_2 + 2\,H_2$$

This reaction is accelerated by the presence of alkali ions, which are sometimes added to the catalysts as promoters, not only to favor this reaction, but also to eliminate support acidity.

3.1.7 Industrial units using Pt-based catalysts

Several commercial processes employ Pt-based catalysts. For example, Oleflex from UOP employs promoted Pt/Al_2O_3 catalysts in a reaction system composed of 3 to 4 moving bed reactors. In this process, the catalyst is continuously regenerated in a separate regeneration circuit. A typical Oleflex catalyst consists of spherical pellets of γ-alumina (surface area about 100 m^2/g) containing Pt (< 1 wt %) and promoted with Sn and alkali metals (e.g. Li). In some patents,[39] it is implied that Co and Zn can also been used as promoters for these catalysts. The STAR process from Phillips Petroleum[40] employs a solid catalyst based on Pt, 0.2 to 0.6 wt %, supported on a Zn aluminate material, 10 to 50 m^2/g. This support exhibits a unique stability at high temperatures in the presence of steam, and this is essential in this case because the process involves the use of steam as a diluent, at a high steam/alkane feed ratio and relatively high pressures, i.e. up to 3.5 atm.. In addition, due to its non-acidic nature, the support does not promote undesired side reactions, such as isomerization or cracking. The catalyst contains Sn as a promoter to reduce coke formation and increases selectivity. As mentioned above, when a diluent such as steam is added, higher equilibrium conversions can be obtained. In this process, the operating alkane conversion at 600ºC is close to 50 % and the overall selectivity is reported to be 95 %.

3.2. Chromia-based dehydrogenation catalysts:

Several oxides are able to readily catalyze the activation of C-H bonds via hydrogen abstraction. In this step, the oxygen species plays an important role in the formation of a surface O-H bond after the rupture of the C-H bond. However, the crucial role is played by the surface cations, which are thought to be responsible for the initial activation of the C-H bond. Chromium oxide has been known as an effective dehydrogenation catalyst for many years.[41] The first chromia-based catalysts were developed at the onset of World War II, when the sources of natural rubber were suddenly discontinued, and butadiene had to be made by dehydrogenating n-butane or n-butene. In recent years, with the increased demand for dehydrogenation processes, modified chromia-based catalysts are being used in the dehydrogenation of isobutane and propane. In industrial applications, alumina is the preferred support. Zirconia has been recently considered as a promising support due to its high thermal and chemical stability.

3.2.1 Kinetics of Dehydrogenation on Chromia Catalysts

Several kinetics studies have been conducted for the dehydrogenation of lower alkanes on chromia-alumina catalysts. A recent study conducted on a commercial catalyst (Cr_2O_3 18 %, Al_2O_3 82%, ZrO_2 0.25 %) has showed that the dehydrogenation of isobutane on this type of catalysts can be described by a Langmuir-Hinshelwood type equation:

$$r_D = \frac{k(P_{iC_4H_{10}} - \frac{P_{iC_4H_8}P_{H_2}}{K})}{(1 + K_{EH}P_{iC_4H_8}P_{H_2} + K_E P_E + K_H P_{H_2})} \qquad (5)$$

Similar to expression (3), obtained for the Pt-based catalysts, this expression predicts a first order with respect to the alkane concentration. However, as opposed to the situation on the Pt catalysts, for which the inhibition by hydrogen was due to a competition for adsorption sites with the alkane, on the chromia catalysts the best fits of the experimental data were obtained when the hydrogen terms in the denominator were neglected. This result is an indication that, on chromia catalysts, hydrogen does not strongly inhibit the adsorption of alkane.

3.2.2. Active Species in Supported Chromia Catalysts

Chromium oxide supported on alumina has been extensively studied by a number of characterization techniques (e.g. UV-Vis diffuse reflectance, Raman spectroscopy, X-ray photoelectron spectroscopy, and chemical analysis). However, the exact nature of the active site is still controversial. The nature of the chromium species existing on the surface of a calcined catalyst are not only dependent on a number of parameters, such as type of support, pre-calcination temperature, and chromium oxide loading, but they also change during the reaction. On a calcined sample, two types of Cr^{6+} species have been normally found. One of them is grafted Cr^{6+}, anchored to the alumina support by interaction with the surface OH groups. The second type of Cr^{6+} species on calcined samples is not chemically bound to the support. The amount of each of these species can be estimated by first extracting the unbound fraction with water, and then titrating (by iodometry) the extracted and solid fractions. The remaining amount of chromium left on the surface is Cr^{3+}. This oxidation state can be either in the form of crystalline aggregates of α-Cr_2O_3, large enough to be detected by XRD, or as highly dispersed Cr^{3+} species,

undetected by XRD. A typical distribution of each of these species as a function of chromium content on a chromia-alumina catalyst series is shown in Fig. 14.[42] It can be observed that, at low chromium loadings, the grafted Cr^{6+} is the dominant species, as the amount of Cr increases, the fraction of soluble Cr^{6+} begins to increase, reaching a plateau at about 2 wt % CrO_3. Interestingly, when the Cr loading was kept constant on alumina supports of varying surface area, the amount of grafted Cr^{6+} increased linearly with surface area. In the present example, at Cr loadings higher than about 4 wt % CrO_3 the Cr^{3+} species begin to form. At the high-loading end, they are the dominant species on the catalyst, including the presence of α-Cr_2O_3, clearly observable by XRD.

In a reducing environment, as that encountered under reaction conditions, the Cr^{6+} species are reduced to Cr^{3+}. Fig. 15a shows XPS spectra of a calcined 15.3 % CrO_3 on alumina catalyst. The peaks obtained in the binding energy region corresponding to Cr 2 $p_{3/2}$ were fitted with contributions from Cr^{6+} and Cr^{3+} states, taking into consideration the multiplet states that arise from the spin-orbit splitting. A significant fraction of Cr^{6+} has been clearly observed in all calcined catalysts, being the dominant form on the catalysts with lower Cr concentration. After a reduction treatment in H_2, or after the dehydrogenation reaction, the peak corresponding to Cr^{6+} decreased significantly. This decrease is illustrated in Fig. 15b, which compares a K-promoted, 15.3 wt % CrO_3/alumina catalyst after calcination, reduction in H_2, and reaction at 470°C in isobutane/He feed. An interesting difference between the two calcined samples in Fig. 15a and 15b is clearly evident. The K-promoted catalyst shows a higher Cr^{6+}/Cr^{3+} ratio, which was also confirmed by chemical analysis and was ascribed to the formation of a potassium chromate phase at the expense of the Cr^{3+} species.

The interesting point is that the Cr^{3+} species are supposed to be the active species, but not all Cr^{3+}species are equally active. In fact, it is believed that the chromium species initially present on the calcined catalyst as dispersed Cr^{6+}, are more active than α-Cr_2O_3. Therefore, the catalyst activation involves the Cr^{6+}-to-Cr^{3+} transformation. However, in many cases, the pre-reduction step is omitted because the reaction environment is reducing and the reaction temperature is normally high enough to induce the transformation. Although a pre-oxidized sample may exhibit a lower initial conversion, it eventually reaches the same conversion as one that has been pre-reduced in hydrogen or other reducing gas.

Industrial chromia-based dehydrogenation catalysts contain small amounts of alkali promoters, typically 1 wt % K. The beneficial role of the alkali is related to its ability to poison the acidic sites on the alumina and to inhibit the undesired cracking and coke formation, associated with acidity. However, the alkali promoter plays a role in determining the nature of the Cr species present on the catalyst surface. As mentioned above, the presence of K may lead to the formation of a potassium chromate (Cr^{6+}) phase. Although this phase is destroyed under reaction conditions, depending on the K and Cr concentrations, its formation may inhibit the generation of less active forms of Cr^{3+}, e.g. α-Cr_2O_3. For Cr concentrations of the order of 15 wt % CrO_3 and above, the addition of K has a promoting effect on dehydrogenation activity, but only at low K concentrations. When the K concentration exceeds about 1.2 wt % K, the formation of the less active α-Cr_2O_3 is enhanced. On the other hand, at low Cr concentrations, e.g. 10 wt % CrO_3 and lower, the addition of K does not result in an increase in activity.

3.2.3 Typical Preparation of a Chromia-based Dehydrogenation Catalyst

The γ-alumina support (surface area 80-100 m^2/g) is impregnated with an aqueous solution of CrO_3 and K_2CrO_4 to derive a loading of chromium of about 5-7 wt % Cr and of potassium of about 1 wt % K. After drying at room temperature, the catalyst is calcined in flow of air at 600ºC for 6 h. During this calcination step, decomposition of the chromium precursors occurs, together with an strengthening in the interaction between the chromium and aluminum oxides. Before reaction, the catalyst is sometimes activated in situ by reduction in hydrogen flow at 500ºC. Alternatively, the reduction can be induced by the reaction mixture. After the deposition of chromium oxide, the surface area typically remains almost unchanged with respect to the original alumina support, which indicates that the chromium oxide does not agglomerate or plug the pores of alumina.

Recent studies indicate that using zirconia (ZrO_2) as a support of chromia catalysts instead of alumina may have interesting advantages. Among the potential advantages of chromia-zirconia catalysts Zirconia is a catalyst support that in recent years has attracted the attention of researchers for applications in several reactions. In most catalyst preparations, the support precursor is hydrous zirconium oxide, which is commonly obtained by precipitation from $ZrOCl_2$ solutions. Typically, the precipitation is carried out by dropwise addition of ammonium hydroxide, or alternatively, by bubbling in the solution a gaseous flow of ammonia in an inert carrier. The precipitate is finally washed to eliminate traces of Cl^-. Without the addition of any promoter, the zirconium oxide rapidly loses its surface area upon heating to the high temperatures required by the dehydrogenation reactions. This loss in surface area accompanies a crystallographic

phase transformation from the metastable tetragonal phase into the monoclinic phase. However, the presence of foreign species, able to interact with the surface of zirconia, significantly retards this transformation and helps retaining relatively high surface areas. This resistance to surface area losses by addition of foreign species has been observed on several systems, such as sulfate zirconia, tungstated zirconia, chromia-zirconia, as well as ceria- and lanthanum-doped zirconias. In all these cases, the preservation of surface area parallels the retention of tetragonal zirconia. Fig. 16 illustrates this trend for a series of chromia-zirconia catalysts. As the Cr content increased, both the surface area and fraction of tetragonal zirconia, retained in the sample after heating at 873 K, increased.

3.2.4. Industrial units using chromia-based catalysts

The three main industrial dehydrogenation processes that employ chromia-alumina catalysts are the Catofin, the Linde-BASF, and the Snamprogetti-Yarsinetz FBD. In the Catofin process, the reaction takes place at sub atmospheric pressure and in the temperature range 525-675ºC in 3 to 8 fixed bed adiabatic reactors, depending on the feedstock. The catalyst is of the chromia-alumina type, containing about 20 wt % chromia. The process does not use hydrogen or steam as a diluent or to decrease coke formation. So, the coking rate is very fast and a cyclic operation is required. Each cycle includes the reaction period, discharge of the reactor, and regeneration/reheating in situ. The regeneration/reheating involves the burning of the coke. This step not only eliminates the coke from the catalyst, but also brings the temperature up, after cooling down due to the endothermicity of the reaction. Typically, about 2 % of the feed goes to coke and the reaction cycles are of the order of 8 min. The complete cycle, including

regeneration/reheating is finished in less than 20 min. Most of the activity is regained after the regeneration/reheating step. However, a slow irreversible deactivation does take place over the reaction-regeneration cycles. This deactivation is due to a decrease in surface area and a phase transformation to the less active form of α-chromia. To compensate for the activity loss, the process temperature is increased, but this temperature increase accelerates the phase transformation and consequently the rate of deactivation. After 1.5 to 3 years the catalyst load has to be replaced.

The Snamprogetti-Yarsinetz FBD process employs fluidized-bed reactors, without diluents and operating at atmospheric pressure. In this process, the chromia-alumina catalyst is continuously transferred from the reactor to the regeneration zone and back to the reactor. The catalyst contains 12-20 wt % Cr_2O_3 supported on a mixture of high transition aluminas.

3.3. Other Lower-Alkane Dehydrogenation Catalysts

In addition to the Pt- and chromia-based catalysts other materials have reported to be active and selective for the dehydrogenation of lower alkanes. For example, zinc titanates have shown moderate activity for isobutane dehydrogenation.[43] These materials exhibit some economic and environmental advantages. Their cost is low in comparison to the Pt-based catalysts and they do not exhibit the toxicity of the chromia-based catalysts. A recent study[44] conducted on zinc titanate films has shown that there is a clear correlation between dehydrogenation activity and the catalyst structure. Depending on the Zn/Ti ratio, several phases may be present on these catalysts. When the Zn/Ti ratio was lower than 1, the phases present were hexagonal zinc metatitanate ($ZnTiO_3$) and

titanium dioxide (TiO_2). At higher Zn/Ti ratios, the main phases were cubic $ZnTiO_3$ and cubic Zn_2TiO_4. The maximum dehydrogenation activity occurred for a Zn/Ti ratio close to 2, whose stoichiometry corresponds to the cubic phase Zn_2TiO_4.

Similarly, sulfided nickel has shown some promising characteristics in the dehydrogenation of isobutane.[45,46] Unlike Pt, unpromoted Ni is very unselective for dehydrogenation reactions. However, even at low dosages S binds very strongly to the surface of Ni and forms stable surface sulfides. When the sulfur concentration is high enough, the typically high hydrogenolysis activity of Ni is eliminated and dehydrogenation selectivity can be very high. One of the interesting characteristics of these catalysts is that not only the dehydrogenation rate exhibits a zeroth-order dependence with hydrogen, but also the rate of deactivation is much less affected by hydrogen than most typical Pt-based catalysts. This difference is probably due to a much weaker interaction of H_2 with the sulfided nickel surface than with typical Pt catalysts.

3.4. Removal of hydrogen to shift equilibrium conversion

The dehydrogenation of lower alkane is in most cases limited by thermodynamic equilibrium. Several approaches have been used to remove part of the hydrogen produced during the reaction from the reacting mixture, thus shifting the equilibrium conversions to higher values. The most promising approaches involve the use of membrane reactors and the addition of hydrogen acceptor materials. For the selective permeation of hydrogen, both inorganic membranes and non-porous Pd membranes have been used in most investigations. Palladium membranes are particularly effective because they only allow the hydrogen diffusion through the membrane due to the high

solubility of dissociated hydrogen in the Pd bulk. The addition of Ag improves the mechanical properties of the membrane, reducing brittleness and modifies the hydrogen solubility, with an optimal performance at about 23 % Ag. A typical membrane reactor configuration[47] employed in the dehydrogenation of lower alkanes is illustrated in Fig. 17. The dehydrogenation catalyst is placed inside the membrane tube. Part of the hydrogen produced by the reaction diffuses out of the reaction zone and it is swept away by a high flow of purge gas that passes by the shell side of the tube. Recent advances in inorganic membranes are opening interesting possibilities to employ these materials in dehydrogenation reactors. For example, combinations of mesoporous Al_2O_3 membranes and microporous silicalite-alumina membranes prepared by hydrothermal synthesis of the silicalite in the host material have been tested with promising results in dehydrogenation reactions. Differences in the permeabilities of hydrogen and the hydrocarbons through these materials are large enough to produce a high permselectivity and dramatic enhances in dehydrogenation conversion.

The second interesting alternative is to conduct the dehydrogenation reaction in the presence of hydrogen acceptor materials. For example, the conversion of isobutane to isobutylene was found to double its equilibrium value in the presence of an intermetallic compound, Zr_2Fe, which is able to form a stable hydride, $Zr_2FeH_{2.6}$. An interesting demonstration of the effect was conducted at 470°C with a chromia-alumina catalyst.[48] In the presence of Zr_2Fe, the initial isobutylene yield was 45 %, which almost doubles the 25 % equilibrium conversion that would be obtained if hydrogen remained in the gas phase. However, after the intermetallic compound was converted into the hydride form, the isobutane conversion dropped to about 20 %.

4. OTHER DEHYDROGENATION REACTIONS

4.1. Dehydrogenation of C_6-C_{19} normal alkanes:

Alkylsulfonate are widely used in industry for the manufacture of detergents and emulsifiers. Dehydrogenation plays an important part in the production of alkylsulfonates, since normal alkanes are an available feedstock, which can be dehydrogenated to the corresponding mono-olefins. In a subsequent alkylation step, the mono-olefins react with aromatics to produce alkylbenzenes, which are finally sulfonated. The typical dehydrogenation of C_6-C_{19} normal alkanes is carried out on Pt-based catalysts at temperatures around 450-520°C. Most of the concepts discussed above for the dehydrogenation of propane and isobutane can be applied for these catalysts. The typical catalyst is Pt supported on alumina, which is promoted with alkali (e.g., Li) to neutralize the acid sites and to improve selectivity and catalyst life. As discussed above, the main cause of catalyst deactivation is coke formation, and one way to extend the life of the catalyst is to co-feed hydrogen at high hydrogen/hydrocarbon ratios. As in the case of lower alkane dehydrogenation the use of promoters such as Sn or In greatly improve the catalyst performance. As opposed to the case of lower alkane dehydrogenation, where side reactions play a minor role, when using higher alkanes, the formation of side products such as aromatics is not uncommon. Therefore, the reaction is operated at low conversions (e.g., lower than 15 %). As a result, the post-reaction separation process plays a very important role. After the dehydrogenation reactor, hydrogen and light alkanes are first separated while the olefins and unreacted alkanes are sent to the

alkylation unit, where the olefins react with benzene to yield the alkylbenzene. After this unit, the unreacted alkanes are recycled to the dehydrogenation reactor.

4.2. Dehydrogenation of Ethylbenzene to Styrene:

Styrene is a major commodity used in the manufacture of plastics, synthetic rubber, resins, and insulators. The principal form of styrene production is the direct dehydrogenation of ethylbenzene, which can be accomplished at around 600-630°C on iron oxide catalysts promoted with various oxides. This process is normally carried out either isothermally or adiabatically in the presence of a large excess of steam, which has several benefits in the reaction. First of all, as shown in section 2 (see Fig. 1), the presence of an inert moves the equilibrium toward higher conversions. Second, the addition of steam supplies the heat required by the endothermic reaction. Finally, the presence of steam at high temperatures helps to inhibit the formation of coke on the catalyst surface.

Among the most common promoters added to iron oxide, the alkali oxides have the most noticeable effects on catalytic activity and selectivity. As illustrated in Table 4,[49] the addition of K in the form of K_2CO_3 causes an increase in activity of about an order of magnitude over the activity of unpromoted Fe_2O_3. This promoting effect reaches a maximum at about 20 wt % K_2CO_3, at higher K concentrations the overall conversion starts decreasing, while the selectivity to styrene slightly increases. The selectivity is typically high. In addition to the main dehydrogenation reaction, some side reactions occur. The most common side reactions are cracking to benzene and ethylene or hydrogenolysis to toluene and methane, and coke formation.

Although several species co-exist in the K-promoted catalysts under reaction conditions, the most active phase is believed to be $KFeO_2$. This phase forms from the interaction of a highly dispersed F_3O_4, mixed with Fe_2O_3, and $K_2Fe_{22}O_{34}$, which acts as a K source.[50] The active $KFeO_2$ phase can be found on the edges of hexagonal platelets consisting of a solid solution of $F_3O_4/K_2Fe_{22}O_{34}$. However, this phase is unstable at ambient conditions, so it is only detected by "in-situ" characterization techniques.[51] Several forms of catalyst deactivation have been identified for this type of catalysts under ethylbenzene dehydrogenation.[52] The first one is the common coke deposition, typical of all the dehydrogenation catalyst. The second type is more unique to this type of catalysts and it is due to the blocking of sites by the CO_2 produced from the reaction of steam with the carbon deposits. These two forms of deactivation are considered reversible because both, coke and adsorbed CO_2, can be eliminated by the same steaming treatment. However, in addition to this reversible deactivation, other irreversible phenomena occur in these catalysts. The most important one is the loss of K from the active phase, $KFeO_2$. This reaction may occur by hydrolysis (with steam) or by direct reduction (with H_2), which results in the generation of KOH. In this form, K can migrate and becomes segregated from the Fe-containing phases. Under industrial conditions, this irreversible process occurs very slowly, and as a result the catalyst life can be of extended to up to two years. To stabilize the active $KFeO_2$ phase other promoters, such as Cr and Ce, have been used, retarding the deactivation process.

References

1. D. B. Kang, A. B. Anderson, *J. Amer. Chem. Soc.*, 107, 7858 (1985)
2. C. Andrews, *Ground Water* 36, 705 (1998)
3. J. Cosyns, J. Chodorge,D. Commereuc, B. Torck, *Hydrocarb. Proc.* 77, Mar. 1998
4. D. E. Resasco and G. L. Haller, in *Catalysis*, Royal Society of Chemistry, Vol. 11, 379
5. F. Buonomo, D. Sanfilippo, and F. Trifiro, in *Handbook of Catalysis*,
6. M. P. Atkins, G. R. Evans, *Erdol, Erdgas, Kohle* 111, 271 (1995)
7. P. Biloen, J. N. Helle, H. Verbeek, F. M. Dautzenberg, and W. M. H. Sachtler, *J. Catal.* 63, 112 (1980)
8. Y. Soma-Noto and W. M. H. Sachtler, *J. Catal.* 32, 315 (1974)
9. L. C. Loc, N. A. Gaidai, and S. L. Kiperman, in *"Proc. IX International Congr. Catal."*, Calgari, Canada, Vol. 3, p. 1261 (1988)
10. F. C. Wilhelm, U.S. Patent 3,909,451 (1974)
11. T. Imai and C. W. Hung, U.S. Patent 4,866,211 (1989)
12. R. D. Cortright, E. Bergene, P. Levin, M. Natal-Santiago, and J. A. Dumesic, *Stud. Surf. Sci. Catal.* 101, 1185 (1996)
13. L. K. Lok, N. A. Gaidai, B. S. Gudkov, S. L. Kiperman, S. B. Kogan, Kinet. Katal. 27, 1365 (1986)
14. R. D. Cortright, P. Levin, and J. A. Dumesic, *Ind. Eng. Chem. Res.* 37, 1717, (1998)
15. R. D. Cortright, and J. A. Dumesic, *J. Catal.*, 157, 576 (1995)
16. G. T. Baronetti, S. R. de Miguel, O. A. Scelza, A. A. Castro, *Appl. Catal.* 24, 109 (1986)
17. S. R. De Miguel, G. T. Baronetti, A. A. Castro, and O. A. Scelza, *Appl. Catal.*, 45, 61 (1988).
18. J. Margifalvi, M. Hegedus, S. Gobolos, E. Kern-Talas, P. Szedlacsek, S. Szabo, F. Nagy, *in* "Proceedings, 8th Inter, Cong. Catal., Berlin, 1984," Vol. IV, p. 903. Dechema, Frankfurt-am-Main, 1984.
19. G. J. Siri, M. L. Casella, G. F. Santori, and O. A. Ferretti, *Ind. Eng. Chem.*, 36, 4821 (1997)
20. R. D. Cortright, and J. A. Dumesic, *Appl. Catal. A*, 129, 101 (1995)
21. A. H. Haner, P. N. Ross, U. Bardi, and A. Atrei, *J. Vac. Sci. Tech.*, 10, 2719 (1992)
22 S. M. Stagg, C. A. Querini, W. E. Alvarez, and D. E. Resasco, *J. Catal.* 168, 75 (1997)
23. H. Verbeek, and W. M. H. Sachtler, *J. Catal.*, 42, 257 (1976)
24. R. D. Cortright, and J. A. Dumesic, *J. Catal.* 148, 771 (1994)
25. D. Rajeshwer, A. G. Basrur, D. T. Gokak, and K. R. Krishnamurthy, J. Catal. 150, 135 (1994)
26. O. A. Barias, A. Holmen, E. A. Blekkan, *Catalysis Today*, 24, 361 (1995)
27. T. B. Massalski, Ed. in *"Binary alloy phase diagrams"*; ASTM. Philadelphia, 1986

28. A. Borgna, S. M. Stagg, and D. E. Resasco, *J. Phys. Chem.* 102, 5077 (1998)
29. Y-X. Li, K. L. Klabunde, and B. H. Davis, *J. Catal.* 128, 1 (1991)
30. Y. Zhou and S. M. Davis, *Catal. Lett.* 15, 51 (1992)
31 J. H. Sinfelt, *Adv. Catal.* 23, 91 (1973)
32 . P. N. Ross, *J. Vac. Sci. Tech.*, 10, 2546 (1992)
33. J. Shen, J. M. Hill, R. M. Watwe, B. E. Spiewak, and J. A. Dumesic, *J. Phys. Chem. B*, 103, 3923 (1999)
34. F. Buonomo, D. Sanfilippo, and F. Trifirò, in "*Handbook of Catalysis"*, p. 2140 (1998)
35 L. Lin, T. Zao, J. Zang, and Z. Xu, Appl. Catal. 67, 11 (1990)
36. T. P. Chojnacki,., and L. D. Schmidt, *J Catal*., 129, 473 (1991)
37. A. El Abed, S. El Qebbaj, M. Guerin, C. Kappenstein, M. Saouabe, and P. Marecot, J. Chim. Phys. 92, 1307 (1995)
38. G. J. Arteaga, J. A. Anderson, C. H. Rochester, *J. Catal.* 184, 268 (1999)
39. G. J. Antos, U.S. Patent 4,216,346 (1980)
40. R. O. Dunn, G. F. Schuette, F. M. Brinkmeyer, W. Sund, *Proc. De Witt Petrochem. Review*, 1992, 1
41. K. K. Kearby, in "*Catalysis"* (P. H. Emmet, editor) Reinhold, New York, Vol. 3 p. 453 (1955)
42. F. Cavani, M. Koutyrev, F. Trifiro, A. Bartolini, D. Ghisletti, R. Iezzi, A. Santucci, and G. del Piero, *J. Catal*. 158, 236 (1996)
43. A. W. Aldag and B. Okla, U. S. Patent 4,524,144 (1985)
44. Z. X. Chen, A. Derkng, W. Koot, and M. P. van Dijk, *J. Catal.* 161, 730 (1996)
45 D. E. Resasco, B. K. Marcus, C. S. Huang and V. A. Durante, *J. Catal.* 146, 40 (1994)
46. D. E. Resasco, B. K. Marcus, C-S. Huang, and V. A. Durante, US Patent 5,468,710 (1995)
47. N. Itoh, *AIChE Journal* 33, 1577 (1987)
48. V. V. Lunin and O. V. Chetina, *Neftekhimiya*, 30, 202, 1990
49. T. Hirano, *Appl. Catal.* 26, 65 (1986)
50. M. Muhler, R. Schlögl, and G. Ertl, *J. Catal.* 138, 413 (1992)
51. M. Muhler, J. Schütze, M. Wesemann, T. Rayment, A. Dent, R. Schlögl, and G. Ertl, *J. Catal.* 126, 339 (1990)
52. K. Kochloefl, , in "*Handbook of Catalysis"*, p. 2151 (1998)

Table 1: Isobutane conversion over a series of Pt and Pt-Sn catalysts. 400 C, 12.5 Torr isobutane, 75 Torr H_2, and 760 Torr total pressure (from ref. 20)

Catalyst	WHSV (h^{-1})	conversion	Pt wt %	total rate (moles iso-C_4/ g Pt h)	selectivity to isubutylene
Pt/SiO_2	6.5	0.190	1.2	1.77	0.20
$PtSn/SiO_2$	3.8	0.042	1.2	0.23	0.98
1:2 Pt-Sn/ L zeolite	3.9	0.053	0.55	0.65	0.88
1:2.5 Pt-Sn/ L zeolite	3.9	0.064	0.44	0.98	0.93
1:3.5 Pt-Sn/ L zeolite	8.2	0.030	0.58	0.73	0.98
1:2 Pt-Sn/ L + K(OH)	3.9	0.069	0.58	0.80	0.99
$Pt/K/SiO_2$	8	0.077	1.2	0.89	0.36

WHSV = (g isobutane/ h) / (g catal.)
Total rate = (moles of isobutane converted/ h) / (g. Pt)
Selectivity = moles isobutylene/moles of isobutane reacted

Table 2: Mulliken Population of the *6s*, *6p*, and *5d* orbitals on three Pt Atoms in Pt and PtSn clusters

cluster	Pt-*6s*	Pt-*6p*	Pt-*5d*
19 atom clusters (constrained)			
Pt_{19}	1.74	1.24	26.60
$Pt_{16}Sn_3$	2.02	1.81	27.22
10 atom clusters (unconstrained)			
Pt_{10}	1.91	1.36	26.67
Pt_6Sn_4	2.40	1.65	27.51

Table 3: Calculated changes in electronic energies (kJ/mol) for adsorption of π-bonded ethylene, di-σ-bonded ethylene, or ethylidyne species on Pt and Pt-Sn clusters

cluster	π-species	di-σ-species	Ethylidyne + H
19 atom clusters (constrained)			
Pt_{19}	- 71	- 116	- 94
$Pt_{16}Sn_3$	- 54	- 87	0
10 atom clusters (unconstrained)			
Pt_{10}	- 103	- 149	- 109
Pt_6Sn_4	- 91	- 91	- 18

Table 4. Effect of K_2CO_3 addition on activity, selectivity, and surface area of Fe_2O_3 catalysts. From Ref. 49

Fe_2O_3 (wt %)	K_2CO_3 (wt %)	Dehydrogenation rate (mol/g min) x 10^5	Selectivity to Styrene (%)	BET area (m^2/g)
100	0	3.2	95.4	15
80	20	33.8	96.6	7.2
75	25	29.6	96.9	6.7
72	28	26.6	96.9	6.3
69	31	24.7	97.0	4.7

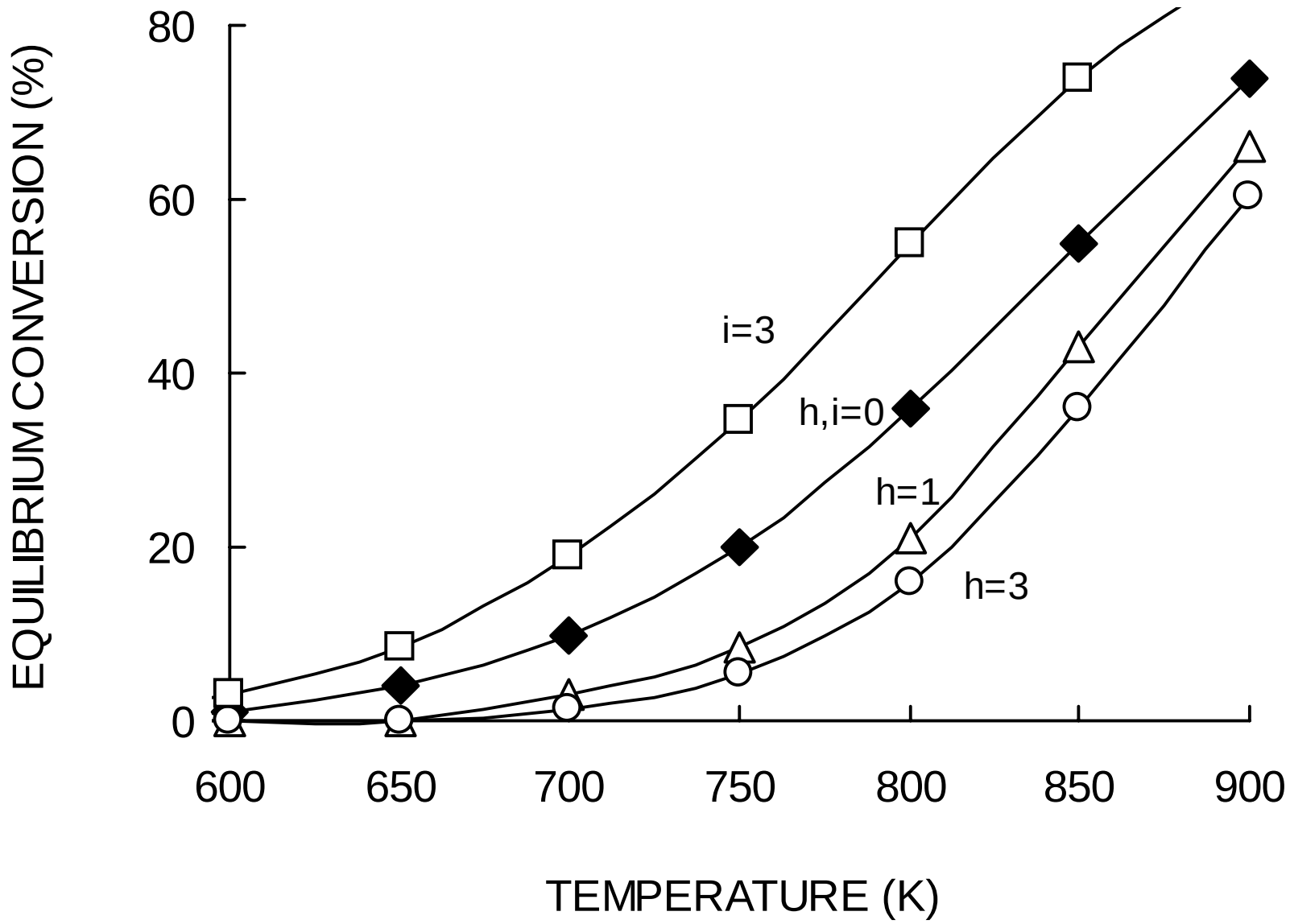
EQUILIBRIUM CONVERSION (%)
80
60
40
20
0
600
650
700
750
800
850
900
TEMPERATURE (K)
i=3
h,i=0
h=1
h=3

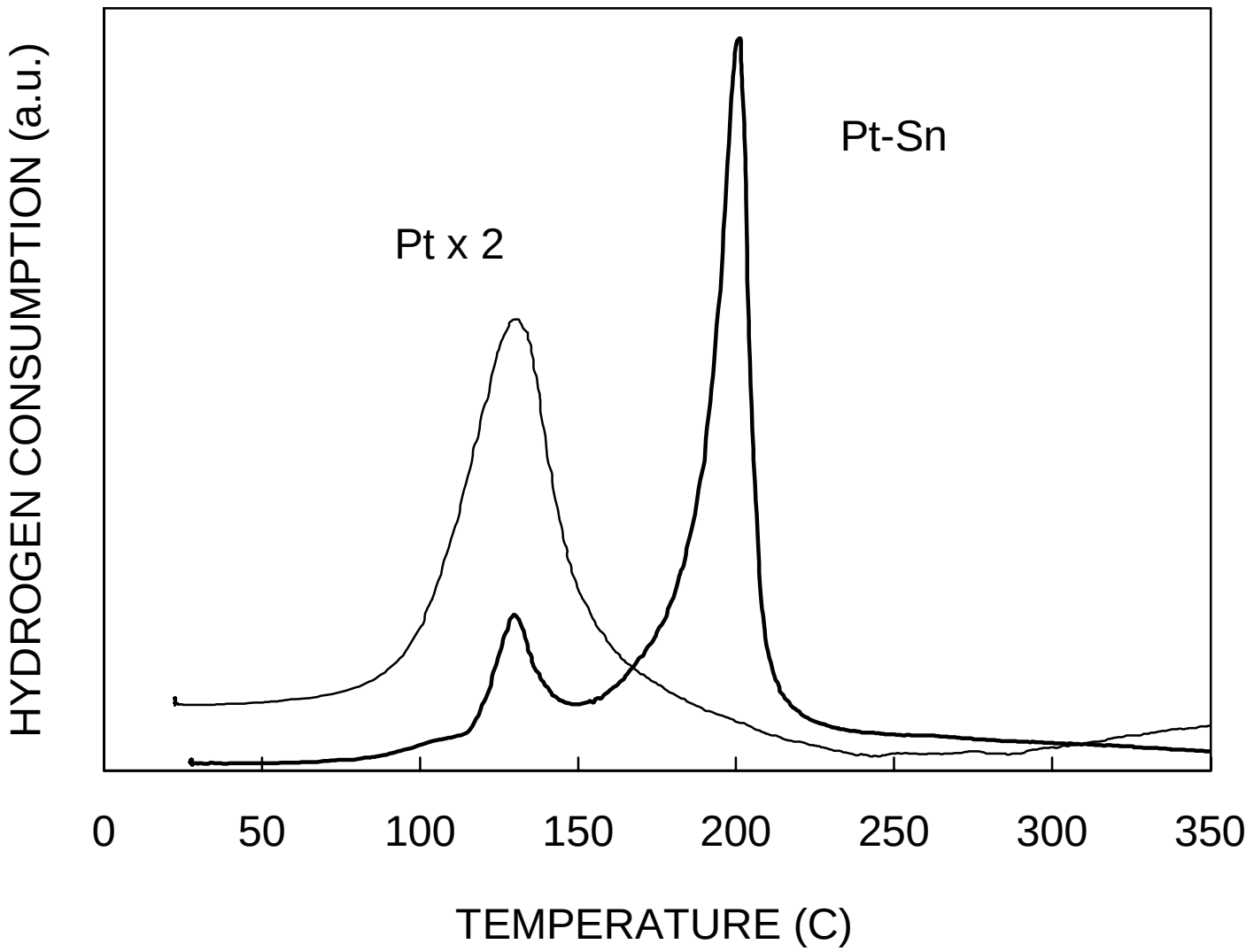
HYDROGEN CONSUMPTION (a.u.)
Pt x 2
Pt-Sn
0
50
100
150
200
250
300
350
TEMPERATURE (C)

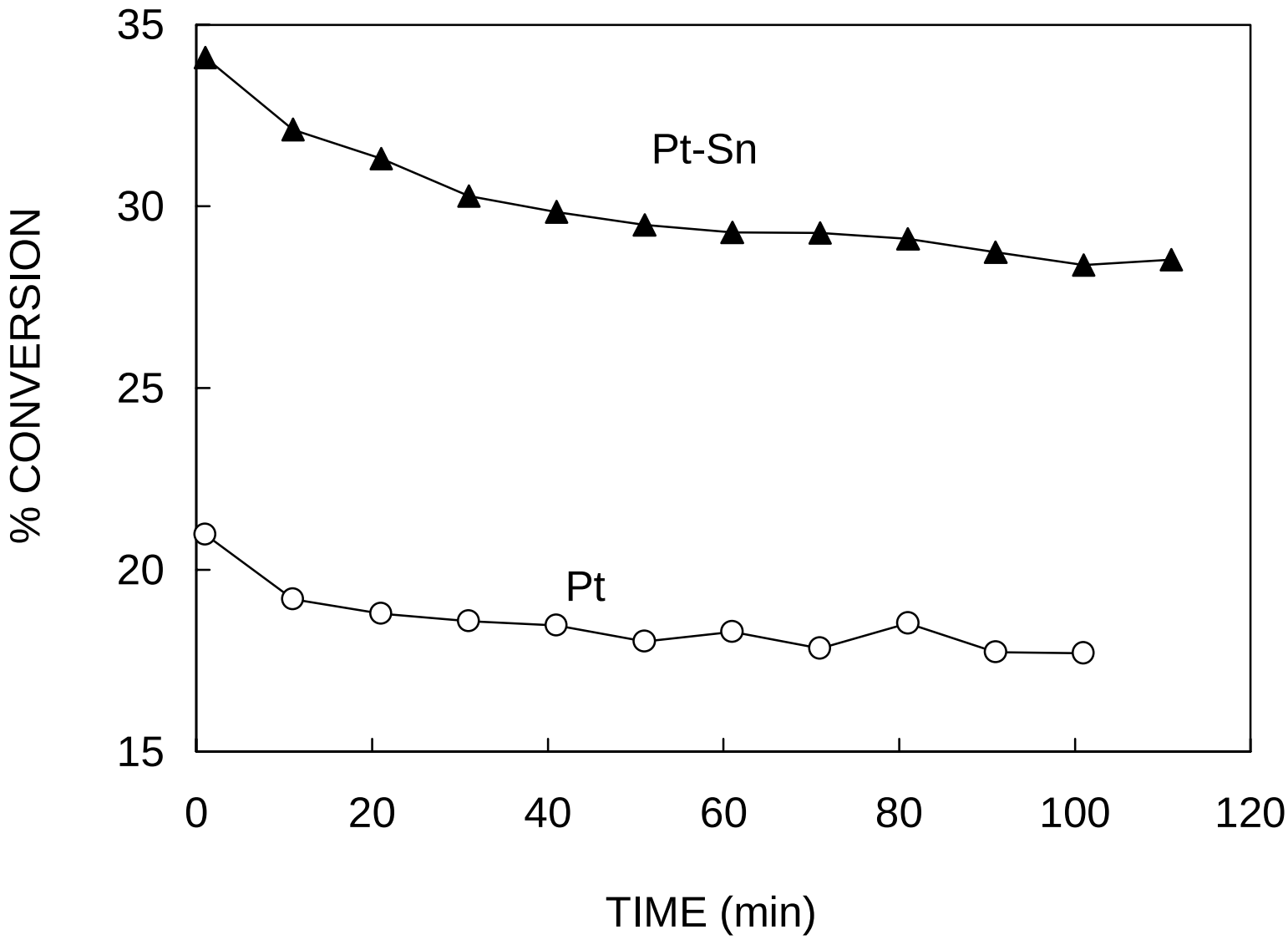
35
30
25
20
15
% CONVERSION
Pt-Sn
Pt
0
20
40
60
80
100
120
TIME (min)

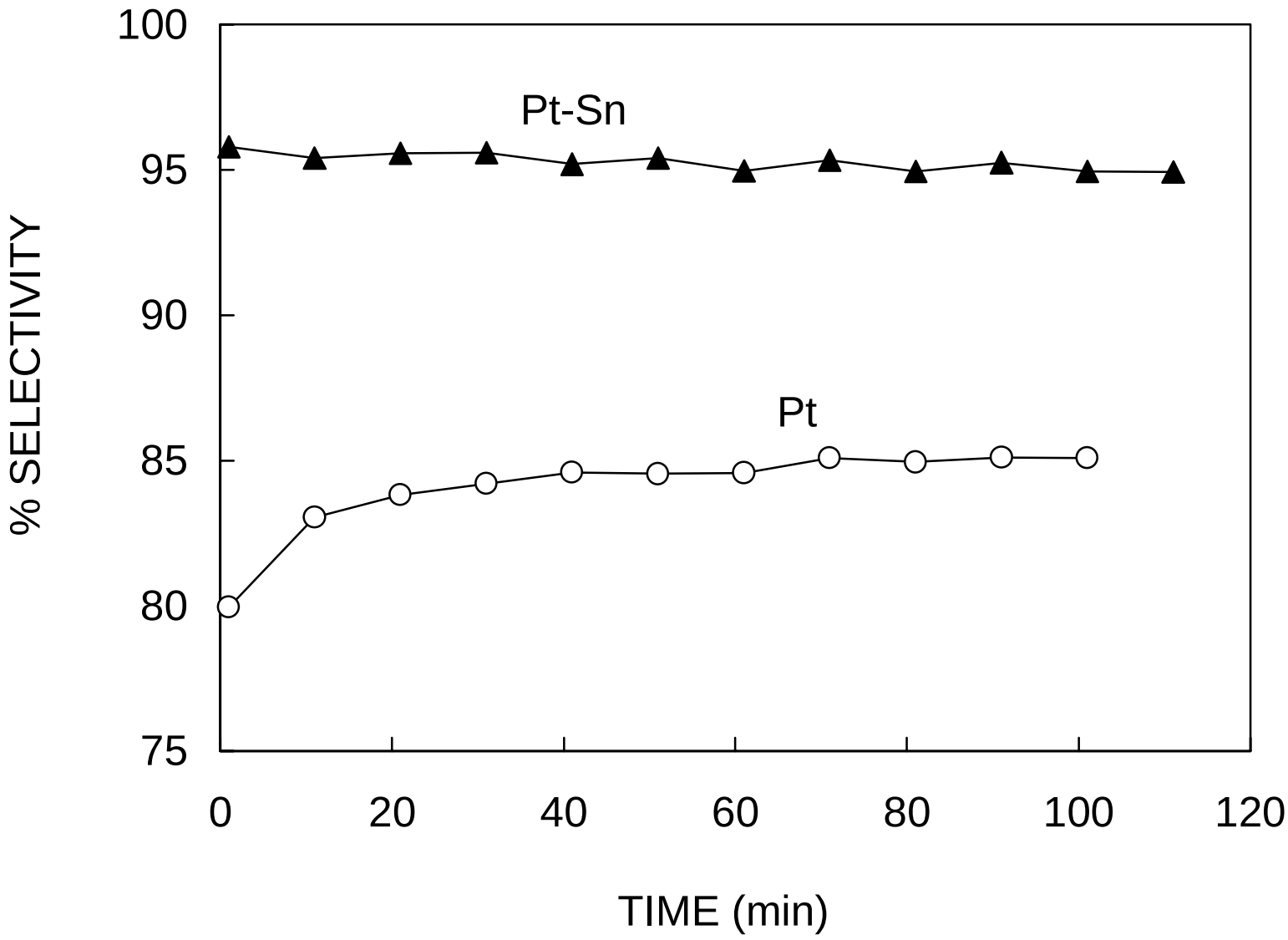
100
95
90
85
80
75
% SELECTIVITY
Pt-Sn
Pt
0
20
40
60
80
100
120
TIME (min)

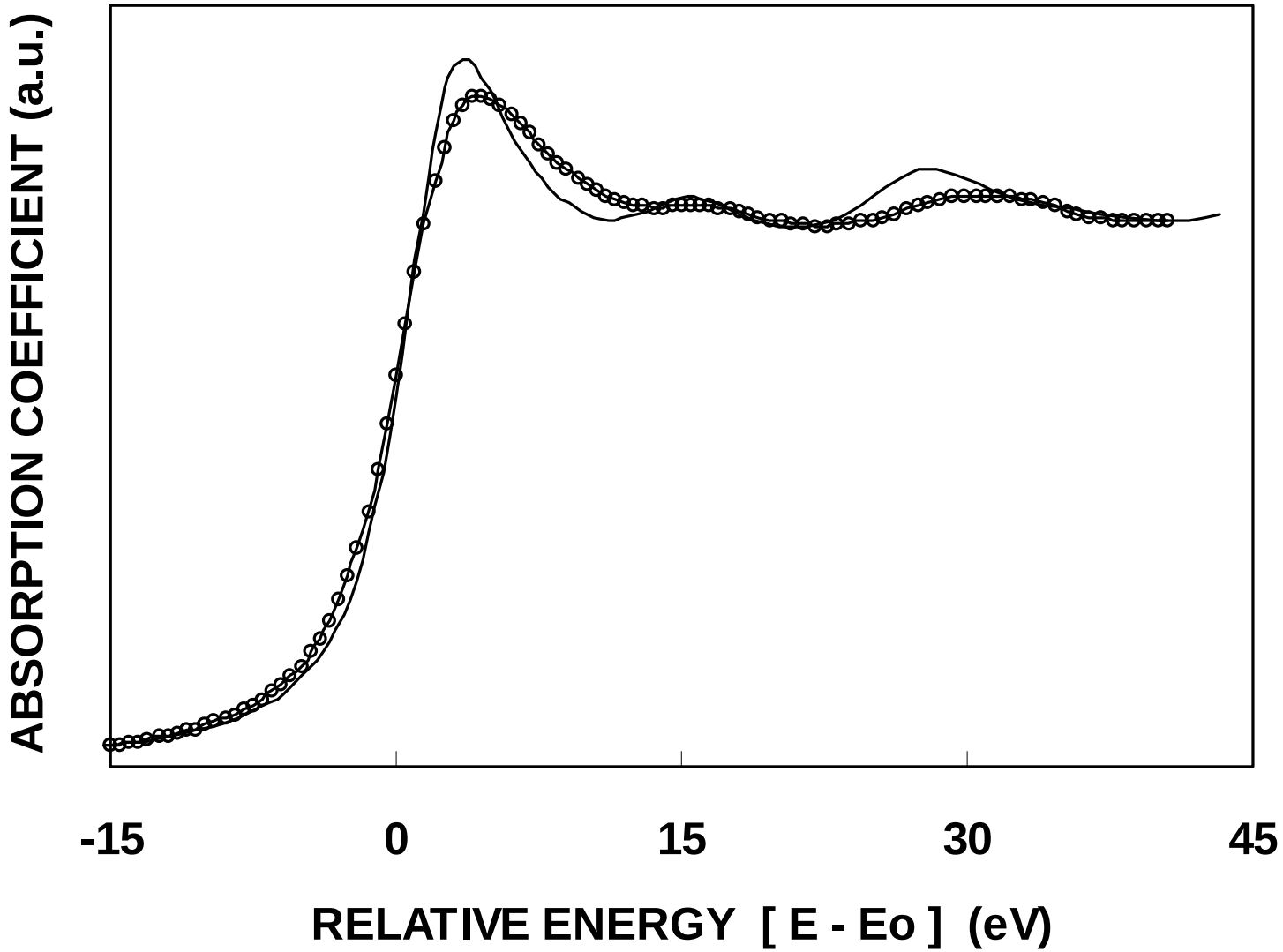
ABSORPTION COEFFICIENT (a.u.)
-15
0
15
30
45
RELATIVE ENERGY [E - Eo] (eV)

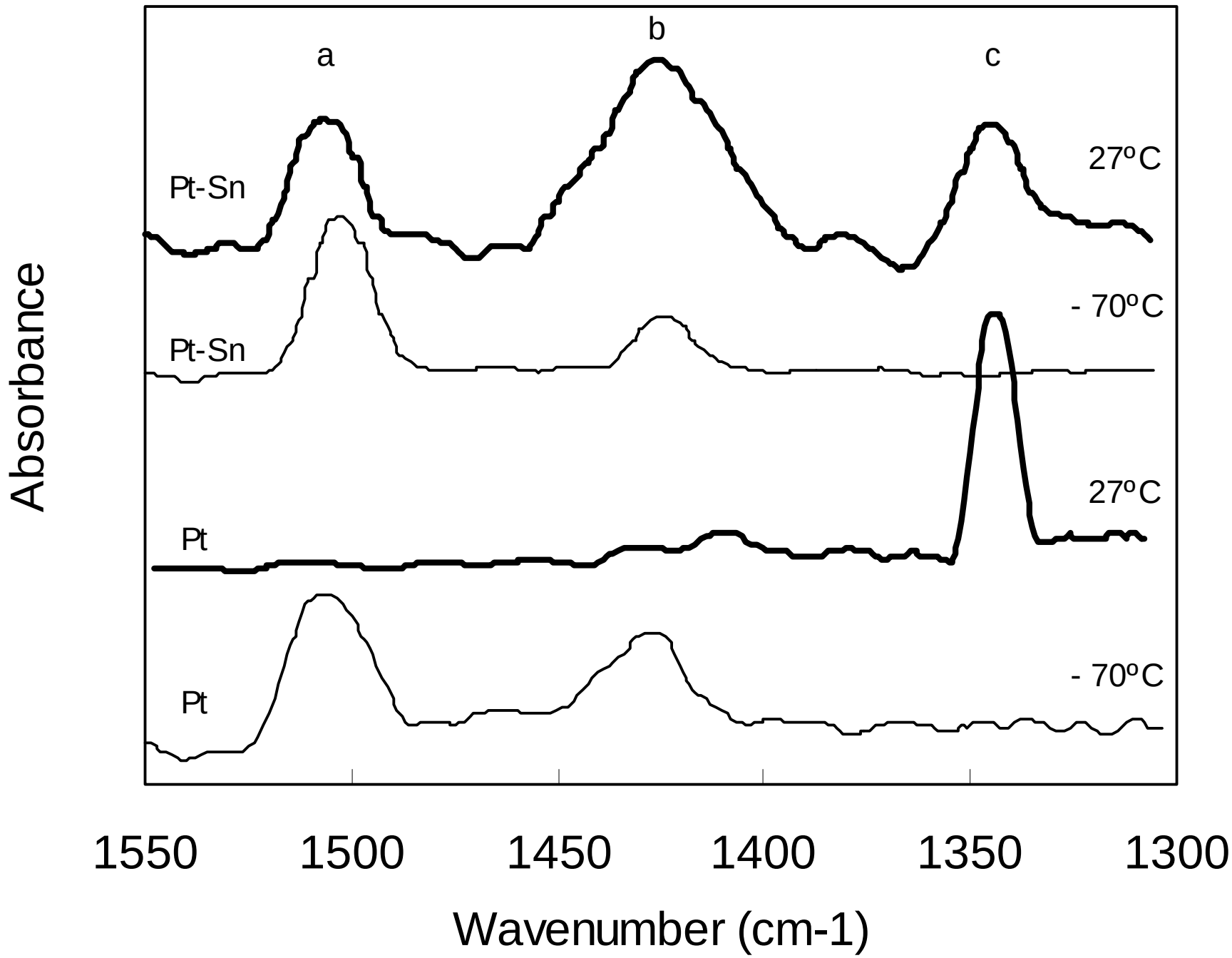
a
b
c
Pt-Sn
27ºC
Pt-Sn
- 70ºC
Pt
27ºC
Pt
- 70ºC
Absorbance
1550
1500
1450
1400
1350
1300
Wavenumber (cm-1)

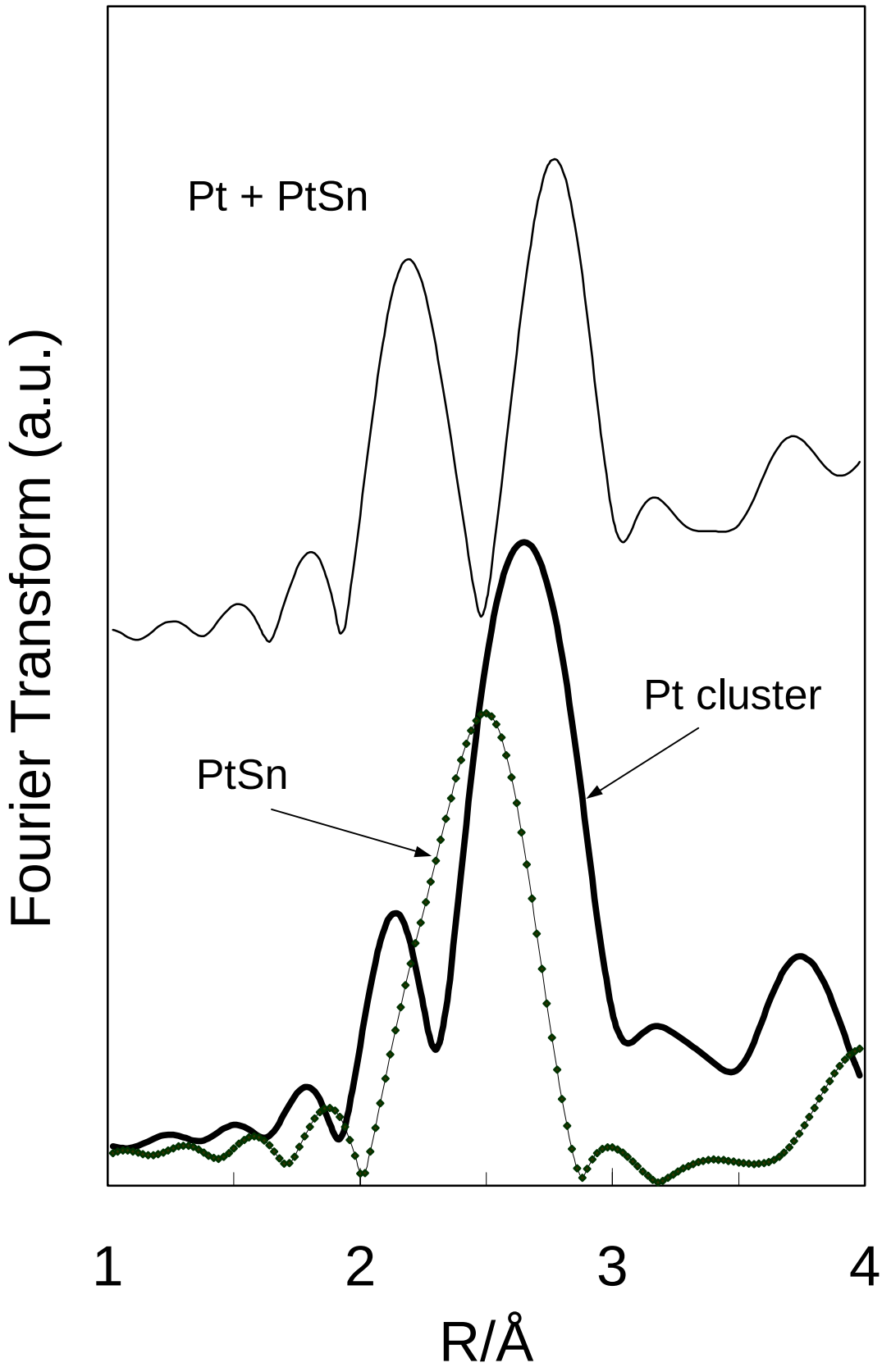
Pt + PtSn
Pt cluster
PtSn
Fourier Transform (a.u.)
1
2
3
4
R/Å

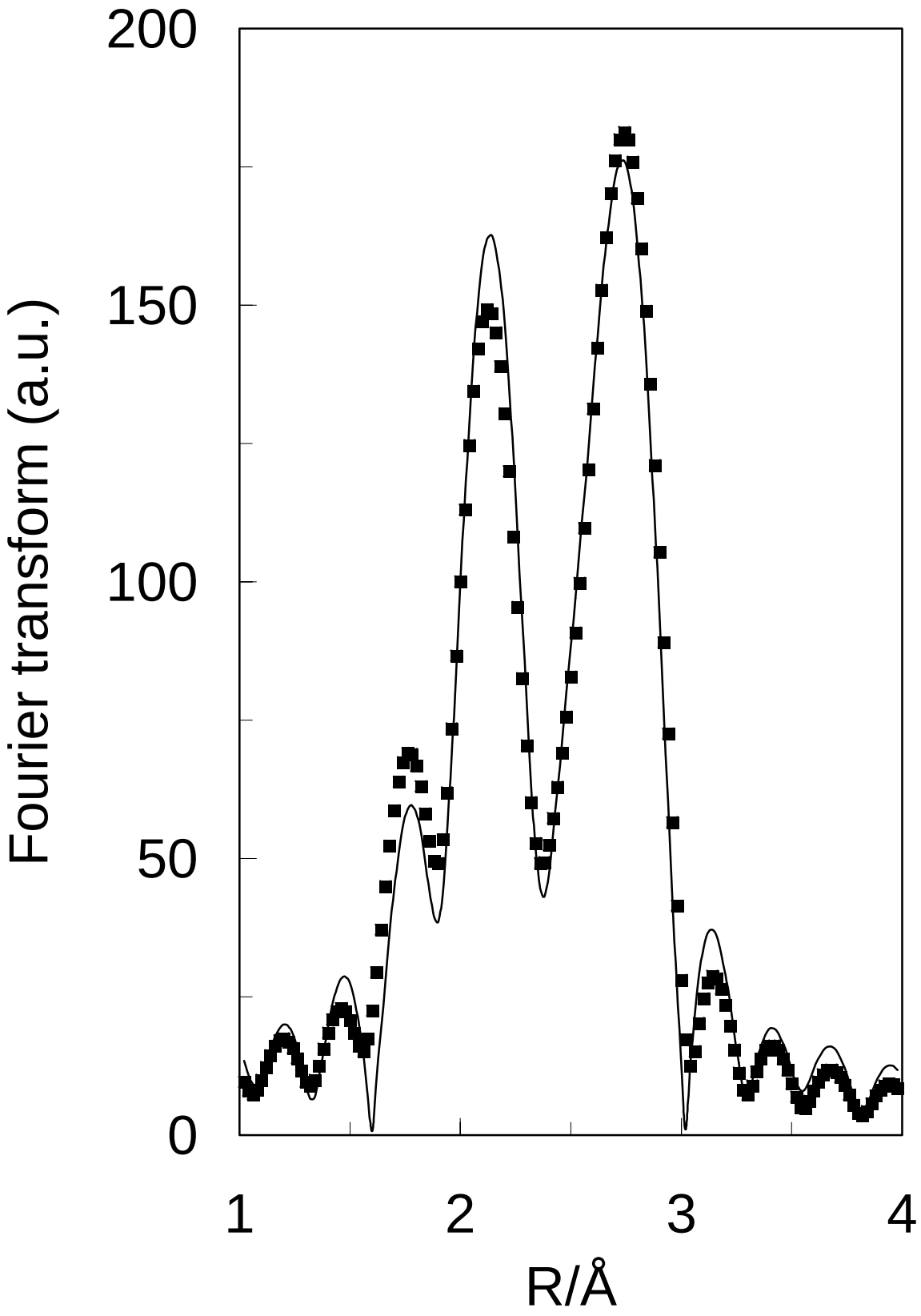
200
150
100
50
0
Fourier transform (a.u.)
1
2
3
4
R/Å

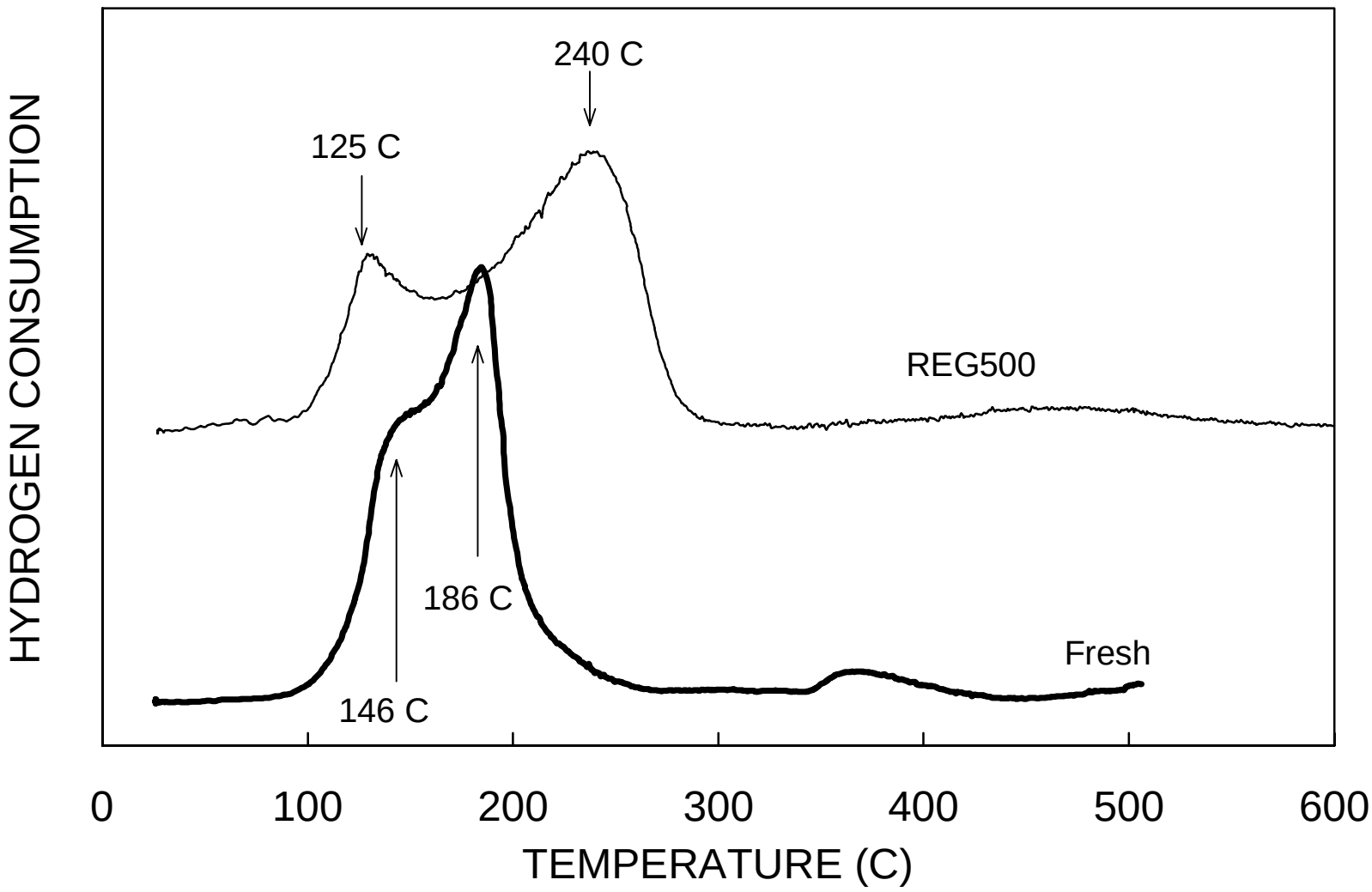
240 C
125 C
REG500
186 C
Fresh
146 C
HYDROGEN CONSUMPTION
0
100
200
300
400
500
600
TEMPERATURE (C)